ACS Catalysis

RESEARCH ARTICLE

pubs.acs.org/acscatalysis

Radical Species Detection and Their Nature Evolution with Catalyst Deactivation in the Ethanol-to-Hydrocarbon Reaction over HZSM-5 Zeolite

F. Ferreira Madeira,*[,†,‡] H. Vezin,[§] N. S. Gnep,[†] P. Magnoux,[†] S. Maury,[‡] and N. Cadran[‡]

[†]LACCO, UMR6503, Université de Poitiers, 40, Avenue du Recteur Pineau, 86022 Poitiers Cedex, France

[‡]IFP Energies Nouvelles, Rond-point de l'échangeur de Solaize, BP3, 69390 Vernaison, France

[§]LASIR, CNRS UMR8516, Université des Sciences et Technologies de Lille, bat C4 F, 59655, Villeneuve d'Asq, France

ABSTRACT: HZSM-5 (Si/Al ratio =16) zeolite was found to be a very stable and efficient catalyst for ethanol transformation into hydrocarbons at 350 °C and 30 bar total pressure. Deactivation, in our operating conditions, was only observed after 16 h on stream, and for ethylene transformation into higher hydrocarbons only. Carbon deposit evolution with time-on-stream (TOS) was fully characterized using IR spectroscopy, GC-MS (after CH_2Cl_2 extraction and HF solubilization), and electron paramagnetic resonance (EPR) techniques. The carbon content was very high from the reaction beginning, leading to great losses of microporosity and acidity. Nevertheless, C_{3+} hydrocarbons yield remained high even after 30 h on stream. EPR analysis allowed us to show the existence of free radical species among the species adsorbed, from the reaction beginning. A decay period of the number of radical species, as well as a change in their chemical nature coincides with the moment of deactivation of the catalyst, leading to a decrease in the formation of C_{3+} hydrocarbons. The existence of reactive radical species could explain the high catalytic performances of the catalyst at 30 h TOS, considering the losses in acidity and microporosity. The apparent correlation between the formation of C_{3+} hydrocarbons and the existence of active radical species could indicate the existence of radical reactions, which should occur at pore mouth. The correlation between the analytical and the catalytic results should be instructive to a better understanding of the deactivation as well as ethanol's transformation reaction mechanism.

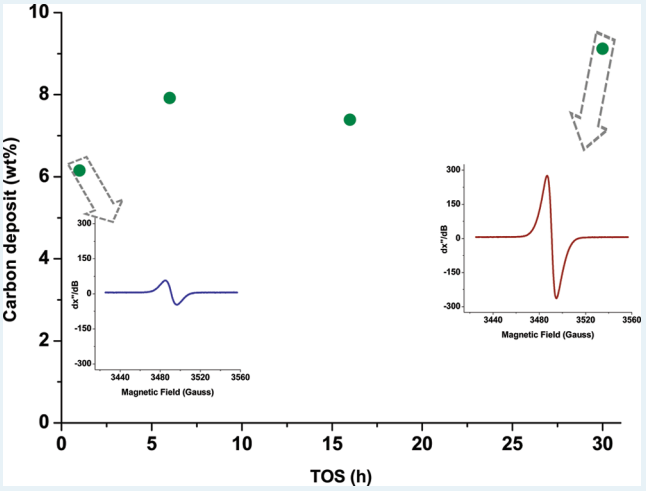

KEYWORDS: ethanol transformation, HZSM-5 zeolites, radicals, EPR, deactivation, hydrocarbons

1. INTRODUCTION

Over the past decades, because of more severe environmental policies and the climb of the oil price, there has been a growing interest in the transformation of biomass as an alternative to fossil fuel.[1−3] Ethanol transformation has become an economically viable alternative, particularly if it does not need to undergo expensive separation processes and can be used in its aqueous form.

Ethanol transformation over solid acid catalyst is well-known for being an easy and fast reaction. HZSM-5 zeolite, widely studied for the methanol transformation, is claimed for being one of the best catalysts for ethanol dehydration into ethylene (bio-ethanol-to-ethylene)[4−10] and into higher hydrocarbons.[3,11−17] Nevertheless, even today, the complete mechanism for ethanol conversion into hydrocarbons was never fully disclosed.

In the case of the Methanol-To-Hydrocarbons (MTH) reaction, the direct route seems to be overruled by the hydrocarbon pool mechanism.[18] The hydrocarbon pool mechanism concept was first introduced by Dahl and Kolboe in the early 1990s,[19,20] but already in the early 1980s Mole and co-workers[21,22] described toluene as playing a role of "co-catalyst" in the MTH reaction over HZSM-5 catalysts. The hydrocarbon pool is generally described by a scaffold composed of larger organic molecules adsorbed in the zeolite. Is has been shown that these adsorbed species are very alike common coke.[23]

More recent studies, over several different zeolites,[24−28] have contributed to clarifying the composition of the hydrocarbon pool. Even in the case of methanol, H-ZSM-5 zeolite, seems to behave differently from the other zeolites, in this case, not only because of its structural characteristics but most likely also because external coking seems to be the cause of deactivation over HZSM-5.[29,30]

The study of the decayed catalysts using several different techniques, such as GC-MS of the extracted carbon deposit, UV DRS, and IR analysis of the coked solids has already proven to be

Received: February 9, 2011
Revised: March 2, 2011
Published: March 07, 2011

a helpful way to the understanding of the methanol transformation reaction.[31] Nevertheless, for ethanol transformation, the catalyst deactivation process and the formation and nature determination of the enclosed species (coke) remains partially unveiled.

One of the least exploited zeolite property in the existing literature is their capacity to spontaneously generate organic cation radicals during the adsorption of organic electron donors. This aptitude is surely connected to the existence of acid sites. These rigid microporous solids are excellent matrixes, stabilizing the cation radicals (which otherwise would be very unstable and reactants), and this is due to the contributions of the strong electrostatic fields inside the zeolite, as well as topological restrictions. The restricted mobility inside the zeolite pores limits the possibility of free radical dimerization and prevents the access for precursor species that typically contribute to the deactivation phenomena.

There are gas phase reactions over acid zeolites where radical cations have been proposed as reaction intermediates (alternative to the conventional carbenium ions path). Examples include Methanol-To-Gasoline over HZSM-5, alkyl benzenes isomerization and dismutation over HMOR, dihalobenzenes ortho-and para-isomerization over metal exchanged zeolites.[23,24,32,33] Aromatic radical cations have also been proposed for the deactivation mechanism and coke formation during benzene oxidation over metal exchanged FAU zeolites.[34]

In our previous study,[35] we have shown, by electron paramagnetic resonance (EPR) analysis, the existence of radical species among the compounds composing the carbon deposit. The HZSM-5 sample tested in that study presented nearly no residual acidity nor microporosity left, even though it remained highly selective in higher hydrocarbon formation.

The present work aims, by using the EPR technique, at enlightening certain aspects such as the possible influence of these radical species on the reaction and products selectivity (radical reaction pathway), and whether this phenomenon is characteristic of only severely decayed catalysts or if these species are present from the reaction beginning. In this study we will combine the use of conventional techniques, such as carbon deposit measurements, IR, and GC-MS, and try to correlate the results with those obtained by EPR analysis (quantification of the radical species as well as determination of the species nature).

2. MATERIALS AND METHODS

HZSM-5 (Si/Al ratio = 16) zeolite is a commercial material from Zeolyst International. The sample was compacted, crushed and sieved to obtain 0.2−0.4 mm homogeneous particles. Before catalytic testing, the solids were activated in situ under a nitrogen flow rate of 3.3 L h^{-1}, at 773 K and a total pressure of 30 bar.

The ethanol used in the catalytic tests was a commercial product from Carlos Erba (96% V/V). It was used without any further purification.

Pore volumes of the fresh and coked catalysts were measured by nitrogen adsorption−desorption with a temperature program starting at 363 K (for 1 h) and rising up to 423 K (coked catalyst) or 623 K (fresh catalyst), under primary vacuum (2×10^{-3} Torr) using an ASAP 2000 instrument (Micromeritics).

Acidity measurements were determined by pyridine adsorption followed by IR spectroscopy using a Nicolet Magna FTIR 550 spectrometer (resolution 2 cm^{-1}). In this case, the samples were first pressed into thin wafers (4−8 mg cm^{-2}) and activated in situ in the IR cell under secondary vacuum (10^{-6} mbar) at 623 K (fresh sample) and 423 K (coked samples). The estimation of acidity by pyridine adsorption was taken at 423 K using ε_B = 1.13 cm μmol^{-1} and ε_L = 1.28 cm μmol^{-1} as extinction coefficients for respectively Brønsted and Lewis acidities.[36]

The carbon content of the coked catalysts was determined by complete combustion at 1293 K under helium and oxygen, using a Thermoquest NA2100.

The CW X-band EPR spectra ($d\chi''/dB$) were recorded on a Brüker ELEXYS 580-FT spectrometer. The Continuous wave (CW) spectra were recorded at room temperature, with 1 G of modulation amplitude and 5 mW of microwave that assumes nonsaturation conditions. 2D-HYSCORE spectra were recorded at room temperature and 4.2 K using the sequence ($\pi/2-\tau-\pi/2-t_1-\pi-t_2-\pi/2-$echo) where the echo is measured as a function of t_1 and t_2, for 4 τ values (88, 128, 200, and 300 ns). The $\pi/2$ and π pulses lengths were, respectively, 16 and 28 ns; the tau value was 300 ns that prevent from the blind spot effects. Signal processing of time domain HYSCORE spectra consists in removing unmodulated echo decay by exponential function subtraction. Then a Fourier transformation of the time domain is performed with a hamming apodization window, and the magnitude spectrum is calculated.

The catalytic tests were carried out in a continuous down-flow fixed bed reactor under a total pressure of 30 bar. The reactor was made of stainless steel, 40 cm long with internal and external diameters of 1.3 and 1.7 cm, respectively. The catalyst (0.3 g) is placed in the middle of the reactor, between layers of glass balls of 1.19 mm diameter. Previous in situ activation was performed under nitrogen (30 bar, 3.3 L h^{-1}) for 16 h at 773 K. The gas flow was kept during reaction, while ethanol (96% V/V) was fed into the reactor at 2 mL/h, which corresponds to a N_2/ethanol molar ratio of 4 and a weight hourly space velocity (WHSV) of 15 h^{-1}. All tests were carried out at 623 K.

Reaction products were analyzed by on line gas-chromatography using a VARIAN 3800 gas chromatograph equipped with two detectors: a FID detector connected to a J&W PONA capillary column (100 m long, 0.25 mm of inner diameter and 0.5 μm of film thickness); and a TCD detector connected to a double column, composed of a 5A sieve (10 m long, 0.32 mm inner diameter and 10 μm of film thickness) plus a Porabond Q (50 m long, 0.53 mm inner diameter and 10 μm of film thickness). The reaction products injection is made under pressure for the FID detector and at ambiance pressure to the TCD detector. The first one allows the detection of all hydrocarbons as well as the oxygenated compounds such as ethanol, diethyl ether, or others. The other one allows the detection of hydrogen, nitrogen, carbon monoxide, carbon dioxide, oxygen, and methane.

The oven programming starts at 293 K (kept for 15 min) thanks to a cryogenic system and rises up to 523 K, with different heating steps at 423 K (kept for 10 min) and 493 K (kept for 34 min), and with a heating rate of 8 K/min.

In addition to the online analysis, the liquid and gas phases are also recovered and analyzed by GC-MS spectroscopy.

3. RESULTS AND DISCUSSION

3.1. Catalytic Results. Under our operating conditions ethanol was totally converted into ethylene, C_{3+} hydrocarbons (hydrocarbons having 3 or more carbon atoms), water (stoichiometric quantity from ethanol dehydration, about 39

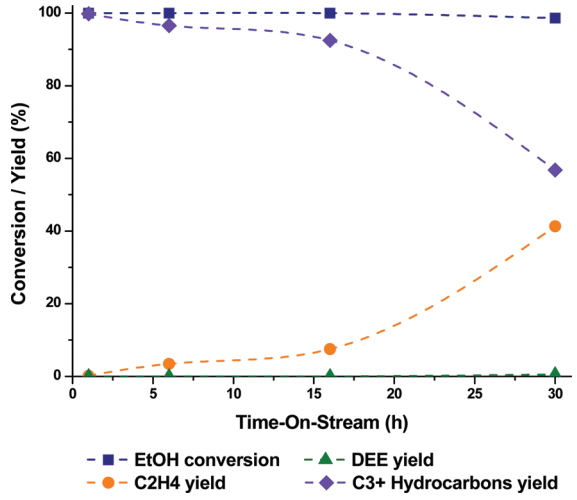

Figure 1. Ethanol conversion and ethylene, diethyl ether, and C_{3+} hydrocarbons yield (wt%) for the 4 experiments at a TOS of 1, 6, 16, and 30 h (Reaction conditions: T = 623 K, P = 30 bar, N_2/EtOH = 4, WHSV = 15 h^{-1}).

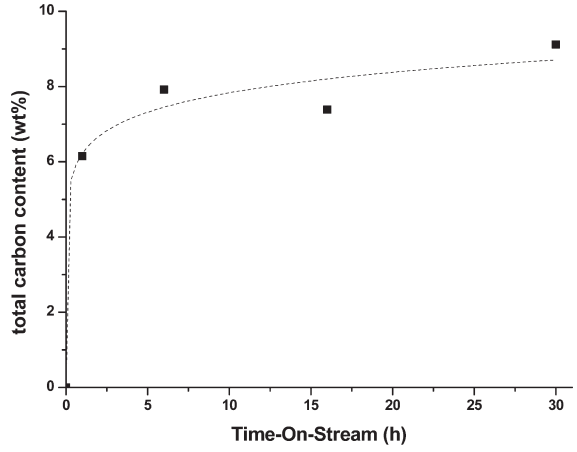

Figure 2. Total carbon content for the four coked H-ZSM-5 (16) samples (TOS = 1, 6, 16, and 30 h). (Reaction conditions: T = 623 K, P = 30 bar, N_2/EtOH = 4, WHSV = 15 h^{-1}).

wt %), and traces of diethyl ether. Initially, ethanol is converted into ethylene and diethyl ether by dehydration reactions, followed by their transformation into higher hydrocarbons, as shown in previous works.[29,35,37]

Four identical catalytic tests were performed under the exactly same experimental conditions and different total reactions times. Reactions were stopped after 1, 6, 16, and 30 h on stream. Ethanol total conversion, primary products (ethylene and diethyl ether) yield, coming from ethanol dehydration as well as C_{3+} hydrocarbon formation yield are shown in Figure 1.

Ethanol conversion was complete, and it remained so for all four runs. Diethyl ether was only detected, under trace form, at the end of the 30 h run. For the 1 h run, all ethanol was completely transformed into C_{3+} hydrocarbons.

The results show that even though there is no deactivation observed for the dehydration reaction with time-on-stream (TOS), there is a deactivation toward the formation of heavier hydrocarbons.

Table 1. Physical-Chemical Characterizations of Fresh and Coked HZSM-5 (16) Zeolite

		acidity* (μmol/g)		pore volume (cm^3/g)		
sample	TOS (h)	Brønsted	Lewis	total	micro	meso
HZSM-5 (16), fresh	0	608	50	0.267	0.184	0.083
HZSM-5 (16), coked	1	71	33	0.093	0.040	0.053
	6	11	13	0.086	0.020	0.066
	16	21	9	0.088	0.030	0.058
	30	3	4	0.063	0.015	0.048

* Brønsted and Lewis acidity measured by pyridine adsorption at 350 °C (fresh catalyst) and 150 °C (coked catalysts).

The higher hydrocarbons (C_{3+}) are mainly paraffinic and aromatic compounds containing between 5 and 11 carbon atoms. This products distribution is further detailed elsewhere.[29]

The catalyst performance and stability for ethanol transformation, under our operating conditions, add some difficulties to the reaction study, and the decayed catalysts study approach seems most fitting to the pursuit our goal.

3.2. Characterizations of the Decayed Catalysts. *3.2.1. Carbon Content Measurements, Residual Acidity, and Microporosity Determination.* Physical-Chemical characterizations of the fresh HZSM-5 (16) zeolite and the four coked samples are presented next.

Figure 2 presents the total carbon content of the four coked samples with their total TOS. A sweeping of the catalyst (immediately after reaction, for about 4 h under nitrogen flow) was performed prior to combustion, to ensure that the amount of carbon measured is only due to coke species. The near vertical slope at the start shows us that the coking phenomena is done very rapidly from the beginning of the reaction, which seems to reach a maximum at about 9 wt % (the step value is most likely determined by the zeolite number of acid sites and pore size and structure of the catalyst). The high carbon content is probably responsible for the deactivation toward the C_{3+} hydrocarbons formation, seen earlier (Figure 1).

The loss of acidity and microporosity (representing 69% of total porosity for the fresh catalyst) is also remarkably fast (Table 1), which is in agreement with the rapid deposit of carbonaceous compounds.

The small amount of mesoporous volume measured could be due to structure defects or to intercrystalline volumes.

We can see that after only 1 h of TOS, the catalyst already presents 88% and 78% loss of Brønsted acidity and microporosity, respectively, even though ethanol is fully transformed into C_{3+} hydrocarbons. With TOS the catalyst reaches a nearly total loss of Brønsted acidity and microporosity, but continues to fully convert ethanol and produces nearly 57% yield of C_{3+} hydrocarbons.

When comparing the results from Figure 2 and Table 1 we observe that at about 16 h reaction there is a slight diminution of the carbon content (Figure 2), which could indicate a certain degree of coke consumption (possible participation of the coke molecules to the aromatic formation) followed by a recoking. This hypothesis is also verified by the Infrared and nitrogen adsorption results (Table 1), which show what seems to be a recovery of acidity and microporosity when comparing to the 6 h reaction sample.

dx.doi.org/10.1021/cs2000686 |ACS Catal. 2011, 1, 417–424

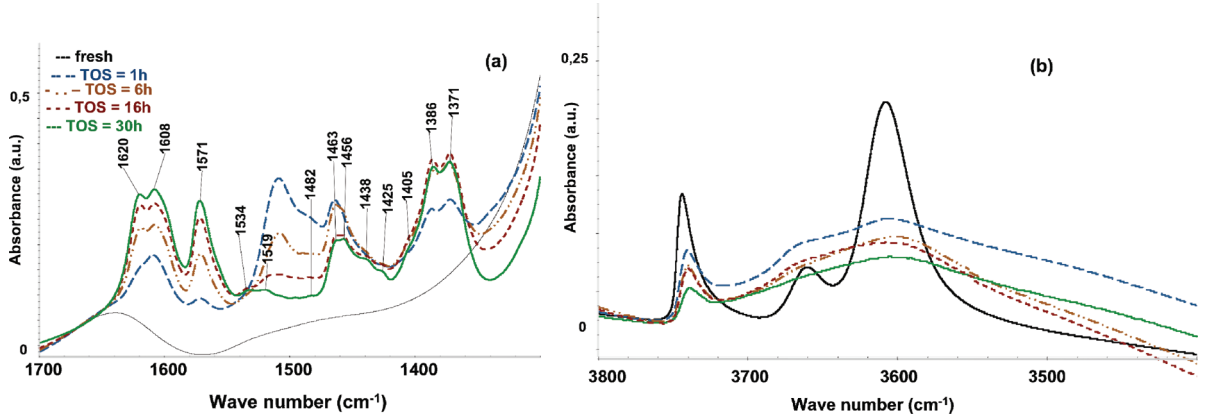

Figure 3. IR spectra for the fresh and all four coked samples (TOS = 1, 6, 16, and 30 h), for the 1300−1700 cm^{-1} (a) and 3500−3800 cm^{-1} regions (b).

3.2.2. Carbon Deposit Nature Analysis by Extraction Followed by GC-MS and IR Analysis. The nature of the molecules composing the carbon deposit was also investigated by IR and GC-MS analysis, and the results compared to the previous characterizations.

IR analyses of all coked samples were performed, and the main vibration bands corresponding to the carbon deposit region (Figure 3.a) and OH region (Figure 3.b) were analyzed and compared to the fresh zeolite.

We can first notice that the vibration bands of the coke molecules region (Figure 3.a) are the same for all coked samples, what changes is their intensity. According to the literature,[38] the vibration bands between 1500−1640 cm^{-1} are generally attributed to the aromatic rings and those between 1350−1470 cm^{-1} are associated with the alkyl branches of the aromatics (CH stretching $\delta_s(CH_2)$, CH stretching $\delta_s(CH_3)$, and/or $\delta_s([CH_3]_2C<)$. This seems to indicate that the compounds occluded in the structure, composing the carbon deposit, are alkylated aromatic molecules. For each sample, the intensities seem to vary, not with the TOS but with the carbon content measured. Nevertheless, the coke molecules nature seems to vary with TOS. The longer the reaction time, the more condensed (polyaromatic) the molecules seem to become (Figure 3a, augmentation of the band near 1600 cm^{-1}, usually attributed to the more condensed aromatics, with diminution of the band near 1500 cm^{-1}, usually attributed to the single ring aromatics).

To be remarked that no oxygenated compounds were detected (no characteristic band at 1700 cm^{-1}).

As can be expected, the presence of coke molecules neutralized OH-bridging acidic bands in the region around 3600 cm^{-1}, but also decreased the intensity of the silanol band (~3740 cm^{-1}, Figure 3b) that usually indicates the existence of external coke.[39] The OH-bridging band (Figure 3b) has disappeared from the first sample, after only 1 h TOS, which again is in agreement with a very fast deactivation mode. As for the silanol band, it gradually diminishes, its decrease being more important with the samples increased TOS. As suggested, external coke, highly polyaromatic molecules that can be formed at the catalyst external surface could be responsible for the silanols bands gradual disappearing.

The carbon deposit was extracted using the method described by Guisnet and Magnoux.[40] In the case of the higher TOS runs (16 and 30 h), a very small amount of occluded material could not be retrieved. This material was attributed to graphitic carbon. Coke molecules recovered by CH_2Cl_2 extraction were then analyzed by GC-MS chromatography. Figure 4 shows the two chromatograms obtained for the soluble coke for the runs TOS = 1 h (Figure 4a) and TOS = 30 h (Figure 4b). We can see that the compounds detected are the same in both cases, what changes are the peaks' intensity. In the 1 h run (Figure 4a) the peaks detected in the first 15 min are more intense that those for the 30 h run (Figure 4b). For the 30 h run chromatogram, the peaks detected in the 23−30 min region are more intense, and were only detected in very small amounts for the sample 1 h run. This already gives an idea of the carbon deposit nature, and it seems to indicate a change in nature with TOS and an increase in the amount accumulated on the catalyst. The first part of the chromatograms (up to about 20 min) corresponds mostly to highly alkylated mono aromatics. These compounds were also detected online by GC analysis during our catalytic tests. For the second part (from 20 to 30 min) more condensed aromatics can be found and still highly alkylated. These compounds are very bulky molecules and are probably responsible for the pore blockage, preventing the reactants access to the interior of the channel (micropore blockage) or for the products formed to come out.

The results obtained by extraction followed by GC-MS, concerning the molecules' nature, are in complete agreement with those obtained before by IR analysis. We can now conclude that the carbon deposit (coke) is composed of highly alkylated polyaromatics.

3.2.3. EPR Analysis of the Samples. By now we have determined the nature of the molecules composing the carbon deposit that leads to the catalysts' deactivation. Even though our analysis shows a strong carbon content and strong losses of Brønsted acidity and microporosity from the reaction beginning (surely because of a carbon deposit composed by bulky alkylaromatic molecules), the catalyst samples continue to show good catalytic performances. This led to the investigation of other properties these molecules might have. In a previous study, we had proven the existence of radical species[34] among the carbon deposit compounds, for heavily coked samples. It is now our goal to investigate the presence/absence of this species from the reaction start and its quantification and to establish a possible connection to the catalytic results. The reactivity of this species could help explain the catalytic results obtained.

The fresh and all four coked samples were first analyzed by the EPR-Continuous Wave (EPR-CW) technique. The spectra obtained are shown in Figure 5.

dx.doi.org/10.1021/cs2000686 |*ACS Catal.* 2011, 1, 417–424

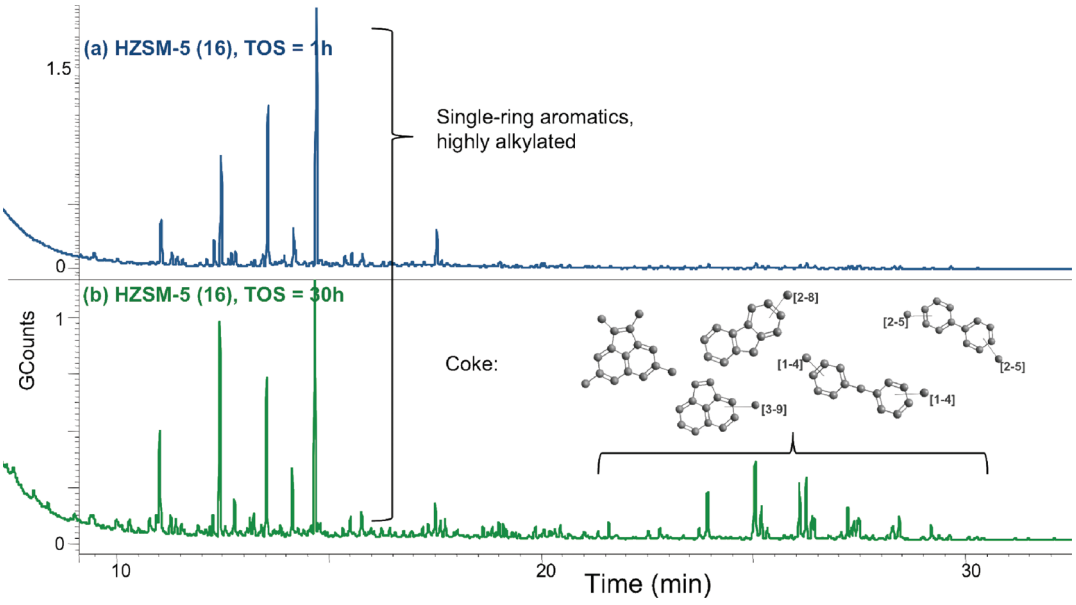

Figure 4. GC-MS analysis of coke molecules extracted by CH_2Cl_2 after solubilization by HF solution, of coked samples HZSM-5 (16) TOS = 1 h and 30 h.

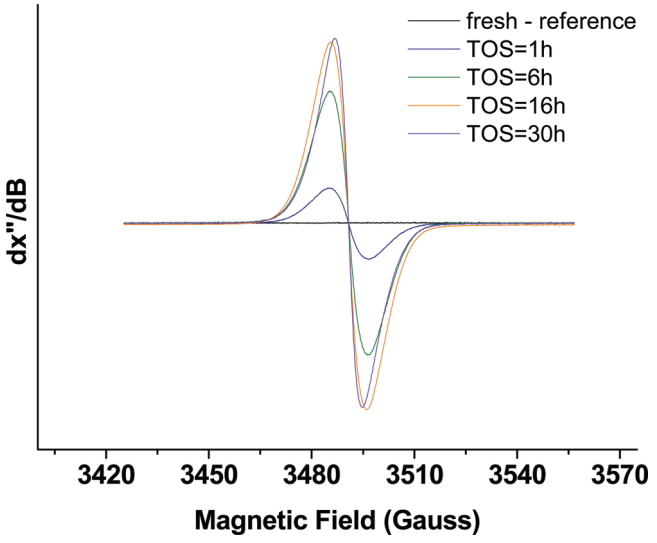

Figure 5. EPR-CW spectra of the adsorption derivative for the HZSM-5(16) samples: fresh and coked (TOS = 1 h, 6 h, 16 h, 30 h).

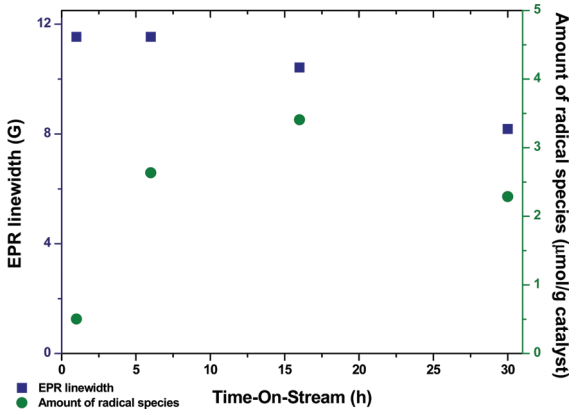

Figure 6. EPR line width and amount of radical species (obtained from spin concentration) for the HZSM-5 (16) samples: fresh and coked (TOS = 1 h, 6 h, 16 h, 30 h).

First of all we can observe that no paramagnetic signal was detected for the fresh sample (which is used as a reference), and therefore, all EPR signals detected on the four other coked samples are due to the existence of paramagnetic species present in the carbon deposit.

Concerning the coked samples, we can observe the existence of a well-defined signal from all samples, meaning the existence/formation of this species from the reaction beginning. All these signals consist in a single Lorentzian line shape centered at a *g* factor of 2.007 and a line width between 10 and 14 G (depending of the sample) assuming an organic radical species. When focusing on the evolution of the signal shape and intensity with TOS, we can observe an increase in the signal intensity from the 1 h to the 16 h TOS sample, which indicates an increase of the spin concentration. When comparing the 16 h and the 30 h signals it seems that we have reached a maximum, but the signal shapes change slightly, becoming thinner. This may indicate a change in the species nature.

To verify this we have represented in Figure 6 the signal width with TOS, as well as the calculated amount of radical species. The amount of radical species was calculated using the Weak Pitch from Brüker as standard reference. The standard (containing a known concentration of spin/mass) was analyzed at the exact same operating conditions, and the spin concentration of the samples is given by the double integration of the first derivative EPR signal.

For a better understanding, the results shown in Figure 6 were divided into three areas. The first area regroups the 1 h and 6 h TOS samples, in which the nature of the species is exactly the same and the amount of radical species increases with time. In the second area, for TOS = 16 h, the amount of radical species grows larger, but also, the species nature starts to change very slightly. In the last part, for TOS = 30 h, we observe a dramatic change, with decrease of the radical species concentration and a change in their nature.

dx.doi.org/10.1021/cs2000686 |*ACS Catal.* 2011, 1, 417–424

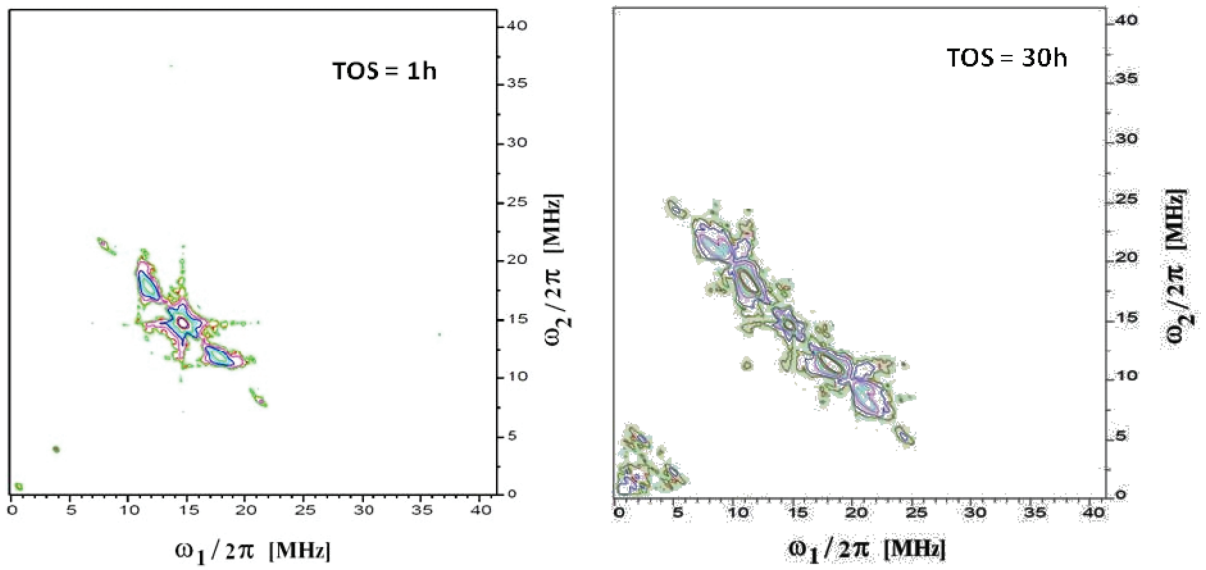

Figure 7. HYSCORE spectra for 1 and 30 h. Spectra were recorded at 4 K with a τ value of 300 ns.

This seems to indicate that, at first, the catalyst has the ability to adsorb/help to form this radical species, and it continues to do so until reaching its maximum capacity (around TOS = 16 h, in the case of this zeolite and under our experimental conditions), forming species of identical nature. We observe then, after reaching the maximum capacity threshold (from TOS = 16 h on), what seems to be an evolution in the radical species nature, very clearly at TOS = 30 h (narrowest line width). To confirm this hypothesis, we have performed some pulsed EPR experiment and particularly the two-dimensional HYSCORE experiment to measure the unsolved hyperfine interaction under the CW EPR line. If the nature of these species changes, it is possible to think that these reactions could concern not only the species itself, but also the C_{3+} hydrocarbons formed. When recalling the catalytic results (Figure 1), the first remark is that the deactivation verified for the C_{3+} hydrocarbons formation occurs simultaneously with the change in the radical species nature. The amount of radical species detected is non-negligible and might be underestimated, as the samples, after catalytic reaction, have been stored for a few months and have been in contact with air, which may lead to the oxidation of the most superficial radical species.

We could imagine a concerted or parallel radical pathway where radical species adsorbed at the pore mouth could contribute to the C_{3+} hydrocarbons formation. When (because of pore blockage chain growth and diffusion cannot occur anymore) C_{3+} hydrocarbons formation is limited to the pore mouth and in the presence of reactive species adsorbed such as radical species, it is highly likely for these species to be involved in the hydrocarbons' formation. The nature change of the radical species can also be due to the growth of the initial species into the formation of a more stable species (less reactive, and bulky enough to stay inside the pore, contributing to coke). This could explain the radical species concentration decrease, the catalyst deactivation, and the coke molecules nature evolution also seen by GC-MS (Figure 4).

To have an idea of the nature of this species at TOS = 1 h and TOS = 30 h, the samples were analyzed by pulsed EPR, using the HYSCORE sequence. HYSCORE spectra are generally represented by four quadrants, two superior and two inferior quadrants symmetric to the first ones. The peaks observed are essentially an NMR spectrum of nuclei that are coupled to the electron. However, the 2D technique allows one to separate overlapping peaks. Peaks appearing in the upper right and lower left quadrants typically arise from nuclei in which the hyperfine coupling is less than the Larmor frequency. They appear at the Larmor frequency, separated by the hyperfine coupling. Peaks from nuclei in which the hyperfine interaction is greater than the Larmor frequency appear in the upper left and lower right quadrants. This will allow having an estimation of the environment surrounding the unpaired electron and the species presumable change in nature. The HYSCORE spectra (right upper quadrant) for the 1 h and 30 h samples are shown in Figure 7.

These spectra, recorded with a τ value of 300 ns interval between the two first $\pi/2$ pulses, show a coupling with the protons whose Larmor frequency is centered at 14.5 MHz. The proton coupling is calculated from the signal extension in the antidiagonal direction. This coupling A is partially composed of a contribution related to the electron delocalization over the coupled nuclei, i.e., Fermi contact term, and another contribution from the orbital recovering which the dipolar part of the A tensor.

On the spectra for the sample TOS = 1 h, we can measure a maximum coupling of 10 MHz for the stronger coupled protons. When we compare the A value for these protons with the 30 h spectra, we can clearly see that this value changes drastically up to 20 MHz. In this case the flat ridge observed arises mainly from Fermi contact term coupling. The number of different couplings also increases. Moreover, in the low frequencies region of the spectrum, we can clearly observe a coupling with aluminum (Larmor frequency of 3.9 MHz along the diagonal) of 5 MHz, of dipolar nature. The aluminum coupling can arise from the orbital overlap of the electron of a radical species with the orbital of the aluminum one in the case of neutral radical species. Also, if the radical formed during the reaction is a radical cation we have to consider the ejected electron that can be localized in the zeolite framework, so in this case these couplings come from the zeolite. In this same area, we can also observe a small ^{13}C coupling of 5 MHz and finally, at around 2.9 MHz, a silicium coupling.

dx.doi.org/10.1021/cs2000686 |*ACS Catal.* 2011, 1, 417–424

The existence of this new coupling at TOS = 30 h, which was not shown for less coked catalysts, shows that the radical species nature changes with TOS. This was also seen by IR analysis, where it was found that the occluded species became "heavier", increasing their carbon number and degree of aromatization. Furthermore, the presence of the aluminum and silicium couplings seems to demonstrate that these radicals are located at the pore interior. This is coherent with the pore volume loss observed. Also, it seems to indicate that any reactions occurring at this time are almost exclusively happening at the pore mouth. These results seem to support the hypotheses of a possible relation between quantity and/or nature of the radical species and the catalytic results (namely, the C_{3+} hydrocarbons formation). The evolution of the nature of the radical species (into more stable/less reactive species, and even becoming heavy coke) seems also to correlate with the decrease in C_{3+} hydrocarbons yield. At higher TOS, these radical species could explain the high activity still observed for the catalyst, but, as seen from the EPR spectra, these species seem to be present from the very beginning. Whether they are not contributing in any way to the formation of C_{3+} hydrocarbons remains indistinct. For instance, if we consider the first step of ethanol transformation, its dehydration into ethylene and/or diethylether, we obtain a C_2H_5 specie adsorbed to an acid center of the catalyst. This specie can easily become a radical specie by spontaneous ionization. One can suppose that if a radical ethyl specie is formed, being a very reactive specie, it could immediately start radical addition reactions leading to the formation of C_{3+} hydrocarbons.

4. CONCLUSIONS

Over HZM-5 (16) and under our operating conditions, all ethanol was successfully transformed into hydrocarbons. Deactivation was observed for ethylene transformation into higher hydrocarbons for reactions times superior to 16 h, while dehydration of ethanol into ethylene was still total after 30 h of TOS. The carbon content after reaction was very high from the beginning (after only 1 h of test), accompanied by great losses of acidity and microporosity. Nevertheless the yield of C_{3+} hydrocarbons remained high. The carbon deposit formed at the beginning of the reaction was determined to be mainly highly alkylated benzenes. The nature of these species was confirmed by IR, GC-MS, and EPR techniques. After 30 h reaction, polyaromatic compounds, characteristic of coke, were detected. This coincides with the change of nature of the radical species detected by HYSCORE, highlighted by the appearance of new couplings at TOS = 30 h. All coked samples presented an EPR signal indicating the existence of radical species among the carbonaceous deposits. The existence of such species could explain the high catalytic performances of this catalyst considering the losses in acidity and microporosity. The amount of radical species, as well as their chemical nature, were studied, and an attempt to correlate them with the evolution of the catalytic results was made. An initial period of formation of similar radical species was observed, until a maximum was reached after 16 h TOS. A decay period of the number of radical species, as well as a change in the chemical nature of those species, coincides with the moment of deactivation of the catalyst, leading to a decay in the formation of heavier hydrocarbons. The new species formed after longer reaction time are more bulky and most probably more stable; therefore we can imagine that they are also less reactive and can evolve to become large coke molecules (observed by the decay in the amount of radical species at TOS = 30 h). This seems to indicate a correlation between the formation of C_{3+} hydrocarbons and the existence of active radical species, which could support the hypothesis of a radical mechanism for the transformation of ethanol. These reactions are most likely to occur at the pore mouth, since the results show almost no microporosity left.

AUTHOR INFORMATION

Corresponding Author

*E-mail: filipa.ferreira.madeira@univ-poitiers.fr.

ACKNOWLEDGMENT

The authors gratefully acknowledge O. Delpoux for his advice.

REFERENCES

(1) Ballerini, D.; Alazard-Toux, N. *Les Biocarburants — Etats des lieux, perspectives et enjeux du développement*; Editions Technip: Paris, 2006.
(2) Cardona, C. A.; Sanchez, O. J. *Bioresour. Technol.* **2007**, *98*, 2415–2457.
(3) Aguayo, A. T.; Gayubo, A. G.; Tarrio, A. M.; Atutxa, A.; Bilbao, J. *J. Chem. Technol. Biotechnol.* **2002**, *77*, 211–216.
(4) Le Van Mao, R.; Nguyen, T. M.; McLaughlin, G. P. *Appl. Catal.* **1989**, *48*, 265–277.
(5) Moser, W. R.; Chiang, C. C.; Thompson, R. W. *J. Catal.* **1989**, *115*, 532–541.
(6) Moser, W. R.; Thompson, R. W.; Chiang, C. C.; Tong, H. *J. Catal.* **1989**, *117*, 19–32.
(7) Nguyen, T. M.; Le Van Mao, R. *Appl. Catal.* **1990**, *58*, 119–129.
(8) Le Van Mao, R.; Nguyen, T. M.; Yao, J. *Appl. Catal.* **1990**, *61*, 161–173.
(9) Phillips, C. B.; Datta, R. *Ind. Eng. Chem. Res.* **1997**, *36*, 4466–4475.
(10) Takahara, I.; Saito, M.; Inaba, M.; Murata, K. *Catal. Lett.* **2005**, *105*, 249–252.
(11) Whitcraft, D. R.; Verykios, X. E.; Mutharasan, R. *Ind. Eng. Chem. Process Des. Dev.* **1983**, *22*, 452–457.
(12) Aldridge, G. A.; Verykios, X. E.; Mutharasan, R. *Ind. Eng. Chem. Process Des. Dev.* **1984**, *23*, 733–737.
(13) Aguayo, A. T.; Gayubo, A. G.; Atutxa, A.; Valle, B.; Bilbao, J. *Catal. Today* **2005**, *107−108*, 410–416.
(14) Schulz, J.; Bandermann, F. *Chem. Eng. Technol.* **1993**, *16*, 332–337.
(15) Marques, J. P.; Gener, I.; Ayrault, P.; Bordado, J. C.; Lopes, J. M.; Ribeiro, F. R.; Guisnet, M. *Microporous Mesoporous Mater.* **2003**, *60*, 251–262.
(16) Saha, S. K.; Sivasanker, S. *Indian J. Technol.* **1992**, *30*, 71–76.
(17) Gayubo, A. G.; Alonso, A.; Vale, B.; Aguayo, A. T.; Bilbao, J. *Appl. Catal., B* **2010**, *97*, 299–306.
(18) Haw, J. F. *Phys. Chem. Chem. Phys.* **2002**, *4*, 5431–5441.
(19) Dahl, I. M.; Kolboe, S. *Catal. Lett.* **1993**, *20*, 329–336.
(20) Dahl, I. M.; Kolboe, S. *J. Catal.* **1994**, *149*, 458–464.
(21) Mole, T.; Bett, G.; Seddon, D. *J. Catal.* **1983**, *84*, 435–445.
(22) Mole, T.; Whiteside, J. A.; Seddon, D. *J. Catal.* **1983**, *82*, 261–266.
(23) Stocker, M. *Microporous Mesoporous Mater.* **1999**, *29*, 3–48.
(24) Mikkelsen, Ø.; Rønning, P. O.; Kolboe, S. *Microporous Mesoporous Mater.* **2000**, *40*, 95–113.
(25) Sassi, A.; Wildman, M. A.; Ahn, H. J.; Prasad, P.; Nicholas, J. B.; Haw, J. F. *J. Phys. Chem. B* **2002**, *106*, 2294–2303.
(26) Sassi, A.; Wildman, M. A.; Haw, J. F. *J. Phys. Chem. B* **2002**, *106*, 8768–8773.
(27) Arstad, B.; Kolboe, S. *Catal. Lett.* **2001**, *71*, 209–212.

(28) Arstad, B.; Kolboe, S. *J. Am. Chem. Soc.* **2001**, *123*, 8137–8138.
(29) Ferreira Madeira, F.; Gnep, N. S.; Magnoux, P.; Maury, S.; Cadran, N. *Appl. Catal., A* **2009**, *367*, 39–46.
(30) Bjorgen, M.; Svelle, S.; Joensen, F.; Nerlov, J.; Kolboe, S.; Bonino, F.; Palumbo, L.; Bordiga, S.; Olsbye, U. *J. Catal.* **2007**, *249*, 195–207.
(31) Palumbo, L.; Bonino, F.; Beato, P.; Bjorgen, M.; Zecchina, A.; Bordiga, S. *J. Phys. Chem. C* **2008**, *112*, 9710–9716.
(32) Chang, C. D.; Hellring, S. D.; Pearson, J. A. *J. Catal.* **1989**, *115*, 282–285.
(33) Tsai, T. C.; Liu, S. B.; Wang, I. *Appl. Catal., A* **1999**, *181*, 355–398.
(34) Hubner, G.; Roduner, E. *Magn. Reson. Chem.* **1999**, *37*, S23–S26.
(35) Ferreira Madeira, F.; Gnep, N. S.; Magnoux, P.; Vezin, H.; Maury, S.; Cadran, N. *Chem. Eng. J.* **2010**, *161*, 403–408.
(36) Guisnet, M.; Ayrault, P.; Datka, J. *Pol. J. Chem.* **1997**, *41*, 1455–1461.
(37) Ferreira Madeira, F. . Ph.D. thesis, Universite de Poitiers, Poitiers, Fance, 2009.
(38) Karge, H. G. In *Introduction to zeolite science and practice, Studies in Surface Science and Catalysis*; van Bekkum, H., Flanigen, E. M., Jansen, J. C., Eds.; Elsevier: Amsterdam, The Netherlands, 1991; Vol. 58, pp 531−570.
(39) Magnoux, P.; Cartraud, P.; Mignard, S.; Guisnet, M. *J. Catal.* **1987**, *106*, 242–250.
(40) Guisnet, M.; Magnoux, P. *Appl. Catal.* **1989**, *54*, 1–27.